

The study of α -alumina scale failure at welded joints in high temperature ODS alloys

P. Muangjunburee and G.J. Tatlock

**Materials Science and Engineering, Department of Engineering,
The University of Liverpool,
Liverpool, L69 3GH, UK.**

ABSTRACT

The high temperature oxidation behaviour of laser welded PM2000, an Oxide Dispersion Strengthened (ODS) ferritic stainless steel, has been studied during cyclic oxidation exposures in air between room temperature and 1050°C, in order to understand the scale failure mechanisms in the vicinity of the joints and further enhance the joint oxidation resistance. The PM2000 laser weld microstructure, oxide morphology, oxide thickness, cracks and spallation were examined using a combination of optical microscopy, scanning electron microscopy and energy dispersive X-ray analysis. The welds and heat-affected zone around the welds were studied in some detail. The results indicated that, although α -alumina scales formed at and near the welds, these regions behaved differently from those in the weld free regions. After a certain period of long-term cyclic oxidation, the surface of the samples started to change colour in the vicinity of the weld. This lighter coloured band spread out from the weld and broadened with time. The oxide scale thickness at the weld was greater than in the regions away from the weld. Convoluted scales, cracks, cavities and small spalled areas were initially observed in the region of local convex curvature located round the periphery of each weld pool. Energy dispersive X-ray analysis did not reveal any compositional change across the scales. The number of cracks in the oxide increased with time and spread out to the rest of the weld and the adjacent area. Tensile stresses normal to the interface generated through scale thickness cracks and lead to spallation after prolonged testing.

Key words:

alumina former, PM2000, Oxide Dispersion Strengthened, cyclic oxidation, spallation.

INTRODUCTION

Oxide Dispersion Strengthened ferritic stainless steels (ODS FeCrAl) have now become regular candidate materials for high temperature industrial applications. The main advantage of ODS FeCrAl alloys over other, more conventional, alloys is the presence of fine, uniformly dispersed and stable yttrium oxide (Y_2O_3) particles, which are incorporated during the mechanical alloying (MA) process. In these alloys, an oxide dispersion produced by the addition of yttria during the high-energy ball milling process contributes to the superior creep strength. This is due to oxide dispersions which act as inhibitors to dislocation motion as discussed by Singer and Art [ref1]. These alloys exhibit not only superior creep strength but also excellent high temperature oxidation resistance. The presence of yttrium oxide (Y_2O_3) particles offers mechanical advantages as well as enhancement of the high temperature oxidation performance. These alloys form a protective α - alumina film above 1050°C and show an adherent scale with low oxidation rate at temperatures up to 1300°C.

Joining is extremely important for the fabrication of components incorporating this alloy. However, welding can damage both the high temperature mechanical and oxidation resistance properties. It is well known that fusion welding often produces inferior mechanical properties, for example, creep and susceptibility to corrosion attack, as shown in [ref2]. Thus, conventional fusion welding processes, such as Tungsten Inert Gas welding (TIG) and Metal Inert Gas welding (MIG) often show agglomeration of oxide particles in the fusion zone of the weld, leading to the generation of a dispersoid free region in the weld and Heat Affected Zone (HAZ). Welding can also change the surface geometry and local roughness that sometimes leads to shorter service lifetimes of welded components due to enhanced surface degradation.

Laser welding, however, is less disruptive of the alloy properties compared to these other welding processes, as reported by Kelly [ref3]. The oxidation behaviour of laser weld joints and the region next to weld has been studied, in order to understand the scale failure mechanisms in the vicinity of the joints with a view to enhancing the joint oxidation resistance.

EXPERIMENTAL PROCEDURE

Raw materials and sample preparation

Pulsed NdYAG-laser welded samples of PM2000 (ODS) alloy were supplied by Plansee GmbH Germany. The composition of the alloy is shown in Table 1. All the samples were chemically cleaned prior to oxidation. This involved ultrasonically cleaning for 20 minutes in methanol, followed by iso-propyl alcohol and analar iso-propyl alcohol.

Oxidation method

Cyclic oxidation was performed using a vertical tube furnace test rig. The samples were oxidized in laboratory air alternately in a hot zone at 1050°C for 15 minutes and in a cold zone (< 90°C) for 10 minutes (25 min. total cycle time). The heating time was 2-3 minutes and the average cooling rate was 100°C/min. The temperature stability in the hot zone is estimated as $\pm 5^\circ\text{C}$ throughout the experiment.

Examination technique

Plan view samples were examined in the optical microscope to study the oxide morphology, initiation and propagation of cracks and scale spallation. For scale thickness investigations, cross-sectional samples were cut from the oxidized alloy, ground successively using 320, 600 and 1200 grits and polished to a mirror finish using 1 μm diamond paste. Optical microscopy, Scanning Electron Microscopy (SEM) and Energy Dispersive X-ray analysis (EDX) were used to evaluate the degradation of the weld and heat-affected zone around the weld in some detail.

Table1 Chemical composition of the major components in **PM2000**

(wt%, Fe- balance)

Cr	Al	Y	Ti	Y ₂ O ₃
----	----	---	----	-------------------------------

19	5.5	-	0.5	0.5
----	-----	---	-----	-----

RESULTS

A low magnification optical image of a fillet weld between a plate and a rod of PM2000 is shown in figure 1. The weld is shown at higher magnification in figure 2 where the individual weld beads can be identified. A cross section through the weld is shown in figure 3 where the microstructure of the components can be discerned. Initial observations after long-term, cyclic oxidation at 1050°C revealed that after a certain minimum exposure time, the surface of the sample started to change colour in the region of the weld. This minimum exposure time varied slightly from sample to sample, but the effect was observed to occur consistently in all the samples oxidised at 1050°C. This lighter coloured band spread out from the weld during additional oxidation cycles, and may be seen clearly in Figure 1, taken after 1773 cycles. The typical relationship between the size of the lighter coloured zone and the number of cycles is shown in figure 4. The precise speed of growth of the lighter coloured zone varied by up to a factor of two between different samples, but was constant for each sample.

Cross sections of samples were mounted and prepared metallographically for the measurement of the protective oxide scale thickness to an accuracy of $\pm 1 \mu\text{m}$ using the SEM. In some areas it was difficult to measure the thickness, since local spalling and/or mechanical damage may have occurred during sample preparation. However, the data indicate that the scale thickness in the vicinity of the weld was greater than in the adjacent regions as shown in figure 5. There was a continuous decrease in oxide scale thickness with distance from the weld region until the lighter coloured region had been traversed. In regions far removed from the weld, the scale thickness was fairly uniform and approximately half the value of the scale thickness measured over the weld.

A convoluted scale and a considerable amount of cracking, both through scale and surface cracking, were observed in the area of local convex curvature of the weld where weld beads had overlapped. Some voids and local spalled regions of oxide were also observed. (figure 6). A lower number of through scale thickness cracks and less local spallation was found over the remaining areas of the weld beads. In some places two layers of scale were observed following the formation of newly grown oxide underneath through scale cracks. In contrast, in the region away from weld, good contact was still maintained between scale and substrate, although there were some cracks present. Energy dispersive X-ray analysis of the outer scale, and the inner scale near the interface between scale and substrate, did not reveal any compositional changes across the layer of oxide.

Cracks, which had initiated and propagated through the scales, were observed by SEM of plan view samples. Comparison of the morphologies of samples after different exposure times showed that cracks appeared on the surface, at the periphery of each weld pool on the weld beads which had a highly convex curvature, after long exposure times (3327 cycles). White spots were found in the secondary electron images at the periphery of each weld pool, and energy dispersive X-ray spectra revealed that these white spots were Y-rich. Furthermore, the SEM images of samples after 4160 cycles indicated that cracks appeared at every periphery of each individual weld pool on the weld bead. After 7000 cycles, cracks were also found within the oxide over the weld beads themselves. Some cracks were found in the oxide over regions adjacent to the welds after longer exposures, as shown in figure 7. SEM plan view images also showed a rougher surface on the weld compared with regions away from weld. Finally after 10000 cycles, a considerable number of cracks were found on the weld and near the weld region. Energy dispersive X-ray analysis then showed Ti rich areas in the vicinity of these cracks.



Figure 1 Low magnification image of the weld geometry, showing a lighter region of oxide surrounding the weld

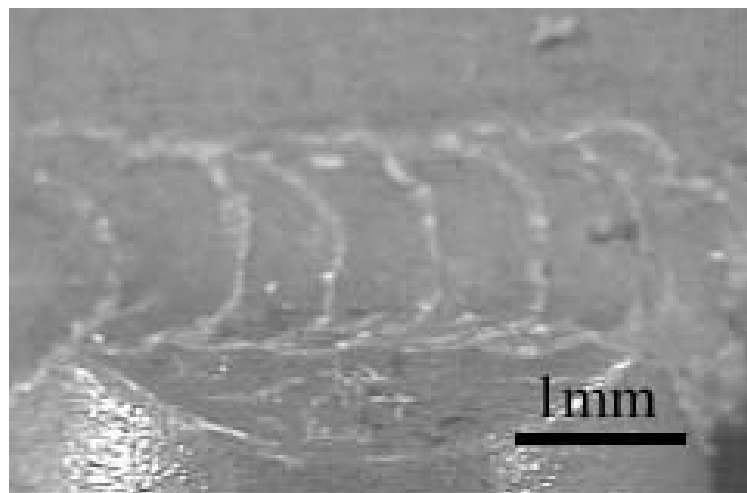


Figure 2 Higher magnification image of the weld beads

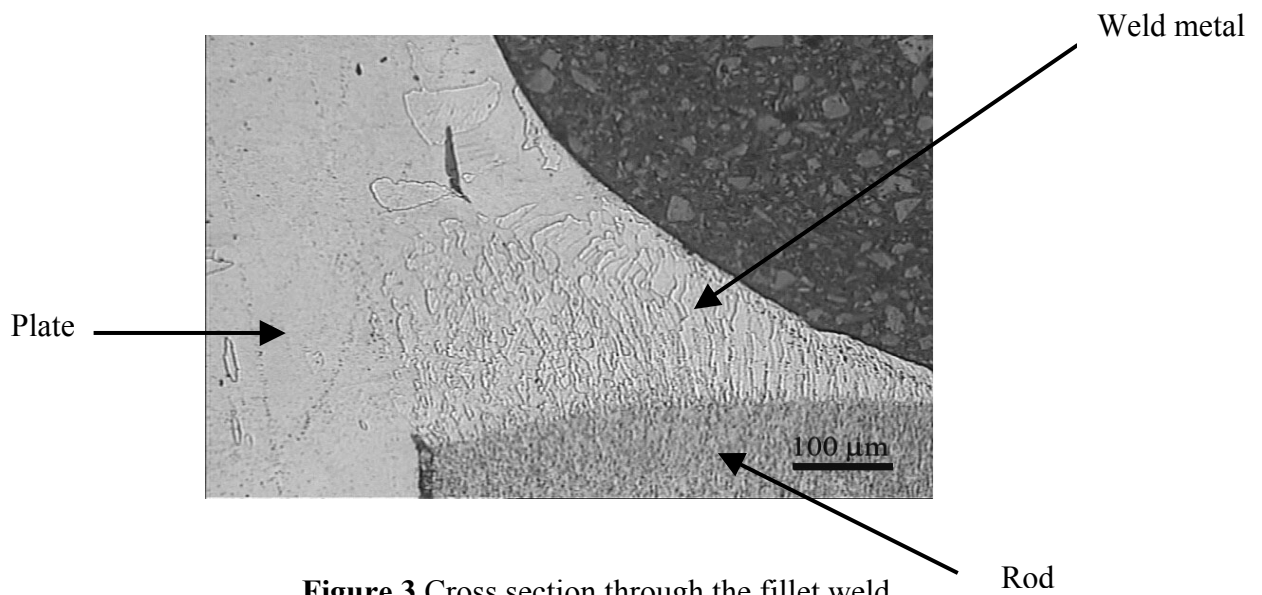


Figure 3 Cross section through the fillet weld

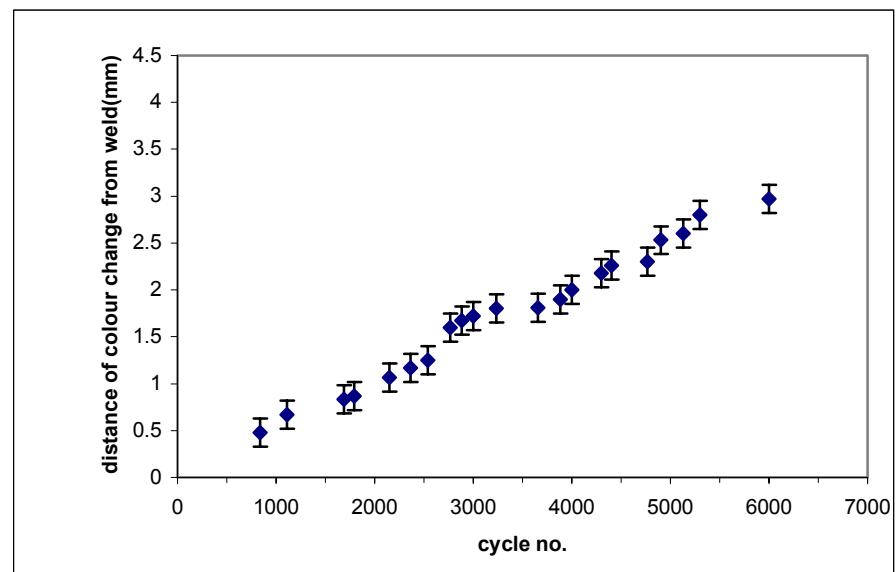


Figure 4 The relationship between the size of the lighter coloured zone and the number of oxidation test cycles.

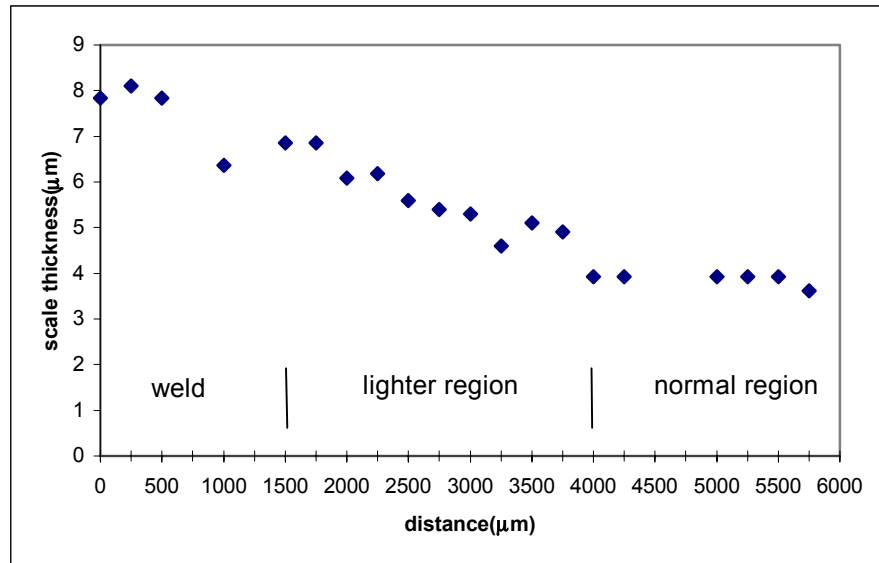


Figure 5 Scale thickness with distance from the weld

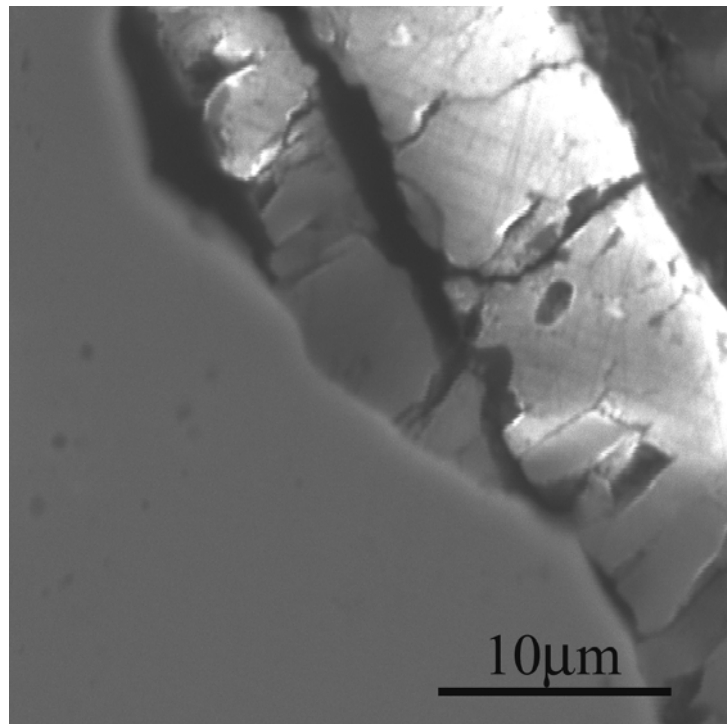


Figure 6 Cross section through the oxide scale over the weld

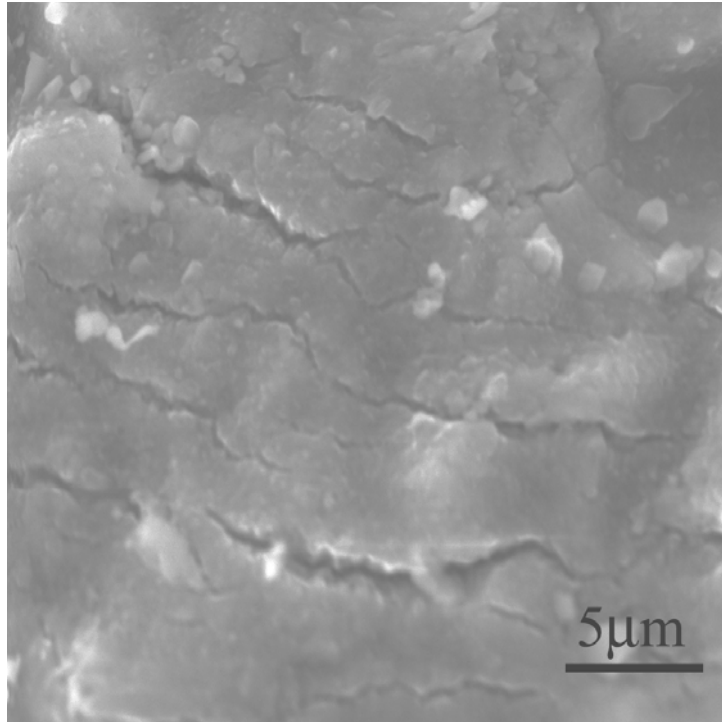


Figure 7 Oxide morphology and cracks in the region adjacent to the weld

DISCUSSION

Although laser welding is a rapid, clean and reproducible method for joining materials, and causes the minimum of disruption to areas of a component away from the weld interface, laser welding of ODS alloys still creates potential problems. Since an area of metal is re-melted and solidified, any oxide dispersion may be re-dispersed or agglomerated and the grain size of the re-solidified material will be different from the grain size of the surrounding material. Hence the high temperature mechanical properties of the weld area may be very different from, and inferior to, those of the surrounding region.

In this project, however, the main emphasis was on the oxidation performance of the component after welding. PM2000 is an α -alumina former at oxidation temperatures of 1050°C, and retains much of its strength at this temperature. Hence only a limited amount of creep relaxation should occur if stresses develop between the oxide and substrate. As the protective scale grows in thickness with time, aluminium is removed from the substrate. However this scale remains intact during cyclic testing, until its thickness exceeds a critical value, when scale spallation commences. If sufficient

aluminium remains in the substrate, α -alumina is reformed in the spalled areas and the alloy remains protected. Once the aluminium level drops below about 2wt%, - the exact figure may depend on several factors, including temperature - the alloy becomes susceptible to breakaway attack with any subsequent cracking of the oxide scale leading to the catastrophic growth of iron and chromium rich voluminous oxides. Hence any premature disruption of the oxide scales in the vicinity of a weld will potentially reduce the lifetime of the component.

Two effects were quickly apparent in this project, during the oxidation testing of rod on plate fillet welds. One was the scale disruption over the weld itself, while the other involved the colour change observed in the vicinity of the weld. Careful examination of the welded area showed that the regions of overlap between one laser melt pool and the next lead to areas with a high local radius of convex curvature, which are impossible to avoid in fusion welding.

It is now well established that the compressive stresses in the α -alumina scale are due to both oxide growth and cooling stresses [ref4,5]. The compressive growth stress can be expected in the α -alumina scale because the Pilling-Bedworth (PBR) ratio of α -alumina is higher than unity and usually the oxide grows by oxygen inward diffusion through the oxide film. In addition, compressive stress can be generated during the cooling of each oxidation cycle. The compressive stresses occurred due to the lower thermal expansion coefficient between α -alumina scale and the substrate.

Previous studies by Schutze [ref6], Evans et al [ref7], and Tolpygo [ref8] have revealed that the residual stresses in the scale strongly depend on the geometry of the substrate and the waviness of the interface. As a result of compressive stress acting parallel to the interface in the scale, the curvature of the surface can lead to tensile and compression stress at the peaks and valleys perpendicular to the interface. From the observation of crack initiation and propagation, they first appeared on the surface at the interfaces between each weld pool. These interfaces have the highest curvature. The tensile stresses are developed at the crest in a direction perpendicular to the interface. It is proposed that the local tensile stresses at the points of local convex curvature exceed the critical value to initiate scale detachment in these areas.

Continued buckling of the scale finally leads to through scale thickness cracks in the area near the base of the ridges. Surface grinding of the welded regions before testing, eliminated most of these ridges and improved the spallation resistance of the samples.

The lightening in colour of the oxidised surface in the vicinity of the weld is more difficult to explain. Figure 4 shows that the position of the interface between the light and dark regions moves away from the weld at an apparently uniform rate (within experimental error). The speed of movement can vary by up to a factor of two from sample to sample, but appears to be constant for a particular sample. The band also spreads out from the weld in all directions, but any anisotropy in the measurements were within the quoted experimental error. Each point on the graph represented the average of four measurements taken in different directions across the sample.

The variation of oxide thickness with position across the sample is shown in Figure 5. In some areas near to the weld, it was difficult to determine this value precisely, because of the convoluted nature of the scale and the spalling and re-healing of the oxide. However, it appears that the average value of the scale thickness over the weld is approximately twice the thickness away from the weld. In the lighter zone adjacent to the weld, the scale thickness decreased in a linear way with distance from the weld, until the boundary between dark and light regions had been reached. Hence this boundary appears to coincide with the edge of the region of thicker oxide.

The colour change may occur for several reasons:

1. Oxide thickness. However, if this was the only factor, then this should result in a gradual colour change with distance from the weld.
2. Impurity diffusion. If impurities diffuse away from the weld with time, and their presence in the scale causes a colour change, then this should result in a parabolic increase in the width of the zone. A more linear rate appears to fit the data. The composition of the oxide also appears to be uniform, as determined by EDX analysis in the SEM.
3. A change in oxide morphology. The nucleation and growth of microcracks or voids in the oxide scale or debonding of the scale from the substrate, could give rise to the colour change and the linear growth of the band with time. The

presence of microcracks or voids could also change the local instantaneous oxide growth rate and hence explain the thicker scales observed closer to the weld, where the mode of growth has been modified for the longest period of time.

The presence of fine cracks in the oxide scale detected by secondary electron imaging in the SEM supports this latter mechanism, but a transmission electron microscope study of the detailed morphology of the scales in different regions is now being attempted, in order to shed further light on the phenomenon. Preliminary results from cyclic oxidation testing at 1100°C also suggest that a lighter band is also formed at this temperature, but that the growth in width of the band is approximately 4 times faster than at 1050°C.

CONCLUSIONS

The welding of ODS FeCrAl alloys can lead to degradation of the mechanical properties of joined components due to dispersoid agglomeration and the different grain structure in the weld pool. The oxidation resistance can also be lowered due to premature scale failure in the vicinity of the welds.

The results of this study on the high temperature oxidation of rod-on-plate fillet welds suggest that there are two separate degradation mechanisms occurring. One is due to the irregular weld geometry and the other is possibly due to stress-induced changes in the oxide morphology in the vicinity of the welds. The former is caused by rough surfaces over the welds, where two weld pools overlap, giving rise to regions of high radius of curvature, and hence high stress fields, leading to premature scale spallation. This can be minimised by post weld machining of the welded joints. The second effect is more subtle, and involves changes to the oxide morphology and subsequent oxide growth rates, possibly induced by extra stresses imposed by the introduction of a weld. Further work is needed to fully explain this effect, but optimisation of the weld geometry, in order to minimise of any extra stresses induced by the constraints of the weld, should reduce the effect and improve the oxidation resistance of the component in the vicinity of the weld.

ACKNOWLEDGEMENT

The authors would like to thank the government of Thailand for financial support of this work. We are also grateful to our partner Plansee GmbH, Germany for the supply of the samples and special thanks to all my colleagues for useful help and discussion.

REFERENCES

- !ref1 'Structure, Processing, and Properties of ODS Superalloy', R.F.Singer, E.Art, Proc. of a conference High Temperature Alloys for Gas Turbines and other Applications pp97-126, 1986.
- !ref2 'Laser welding of oxide dispersion strengthened alloy MA 754, P.A. Molian, Y.M. Yang, P.C. Patnaik, Journal of Materials Science, 27, pp2687-2694, 1992.
- !ref3 'Pulsed YAG Laser Welding of ODS Alloys', T.J. Kelly, Proceeding of Symposium on Laser-Solid Interactions and Laser Processing, Boston, Material Research Society, pp215-220, December 1978.
- !ref4 'The modelling of growth stresses during high temperature oxidation', F.H. Stott, A.Atkinson, Materials at high temperature, 12, pp195-207, 1994.
- !ref5 'Scale growth and stress development', A.M.Huntz, Materials science and Technology, 4, pp1079-1088, 1988.
- !ref6 'Stresses and decohesion of oxide scales', M. Schutze, Materials Science and Technology, 4, pp407-414, 1988.
- !ref7 'On the Mechanical Behaviour of Brittle Coating and Layers', A.G. Evans, G.B. Crumley, R.E. Demaray, Oxidation of Metals, 51, pp193-216, 1983.
- !ref8 'The Morphology of Thermally Grown α -Al₂O₃ Scales on Fe-Cr-Al alloys', V.K. Tolpygo, Oxidation of Metals, 51, pp449-477, 1999.